EDLC Technology for Energy Storage from Materials to Application: A Comprehensive Review

Won-Chun Oh[1†]

Department of Advanced Materials Science & Engineering, Hanseo University, Seosan-si, Chungnam-do, Korea, 356-706

Abstract: Based on previous reports, the key factors that dictate the selection of electrode materials for ECs are the following: (1) high SSA, leading to the large capacitance; (2) suitable surface functional groups to enhance the capacitance by additional faradaic redox reaction and improve the wettability; (3) large pore size, short pore length, and straightforward pore connectivity to facilitate the ions diffusion with a high speed; (4) low internal electric resistance, which leads to fast charging-discharging and low ohmic resistance; (5) low volume and weight; (6) low price; (7) environmentally friendly materials; (8) thinner electrodes and current collectors. carbon-based materials with macro-, micro- and nano-structures have been applied to construct various attractive electrochemistry energy devices, sorbents and catalysts. A variety of methods including hydrothermal/solvothermal reaction, self-assembly, organic sol–gel reaction and template guided growth have been developed for preparing carbon based materials. So there is tremendous room available in the design and synthesis of novel carbon-based materials for energy-related applications. Although some literatures indicated that carbon-based materials products have prominent ability in the field of pollutants detection and environmental remediation. There are a lot of pollutants and microorganism that exist in circumstance, and only a small part of them have been explored. Thus, the mechanisms of pollutants detection and removal based on multifunctional carbon-based materials need to be further developed. Porous carbon-based materials with the porosity and flow characteristics can be applied for flow-through reactors in separation and catalytic processes. The safe operation and "green chemistry" in environmental protection should also be considered for practical applications.

Key wards: EDLC, carbon based materials, energy storage, electrochemistry, green chemistry
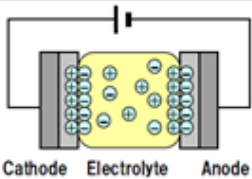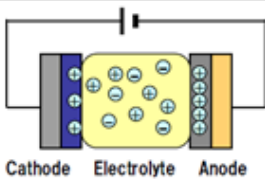
1. Introduction

Electric double layer capacitors (EDLCs) have attracted much attention as an electrochemical energy storage device due to their high power density and long durability [1-5]. Supercapacitors are considered as one of the most promising electrochemical energy storage

† Corresponding author. Tel: +82-41-660-1337; Fax:+82-41-688-3352; E-mail: wc_oh@hanseo.ac.kr

devices of the present century [6-8]. They have higher power densities and exceptional long cycle life than conventional batteries and higher energy densities than conventional dielectric capacitors. Based on charge storage mechanisms, supercapacitors are broadly classified into two categories viz, lectrochemical double-layer capacitors (EDLCs) and pseudocapacitors [9,10]. While in EDLCs, energy storage takes place by ion adsorption between electrodeeelectrolyte interface, pseudocapacitors store energy by fast and reversible Faradic reactions. Carbon based materials such as activated carbon, mesoporous carbon and graphitic nanocarbons (nanocoils, nanofibers, nanotubes, nanocones, etc) are widely used as electrode materials for EDLCs [11,12]. Commonly used electrode materials for pseudocapacitors are transition metal oxides and conducting polymers [9,13].

Table 1
Comparison of charge storage.

	Electric double layer capacitor (EDLC)	Lithium ion battery (LIB)
Structure	Cathode Electrolyte Anode	Cathode Electrolyte Anode
Cathode material Anode material	Activated carbon Activated carbon	Lithium metal oxide (LiCoO2) Carbon (Graphite)
Storage mechanism	Ion adsorption-desorption on surface (Physical reaction)	Li-ion intercalation- deintercalation in active material (Oxidation-reduction reaction)
Energy density	△ ($\sim$10Wh/L)	◯ ($\sim$550Wh/L)
Quick charge-discharge	◯ (msec order)	△ (Charge:100min/Discharge:10min)
Cycle life	◯ ($\sim$100k cycle)	△ ($\sim$1k cycle)

A number of carbon materials, such as activated carbons [13-15], carbon nanotubes [16-20], and carbon aerogels [21-25], have been widely used as electrode materials for EDLC. Among the various carbon materials, activated carbons are mainly employed as the electrode material for EDLC in the commercial industry due to their high surface area, chemical and thermal stability, and low cost [26,27]. However, it is well known that the activated carbons retain abundant micropores (<2 nm), which are not easily wetted by the organic electrolyte ions [27]. In addition, the ionic motion may be limited in such small pore during the charge/discharge at high current density [27]. Therefore, it is expected that carbon materials with a high surface area and well-developed mesopores (2-50 nm) will serve as efficient electrode materials for EDLC in organic electrolyte.
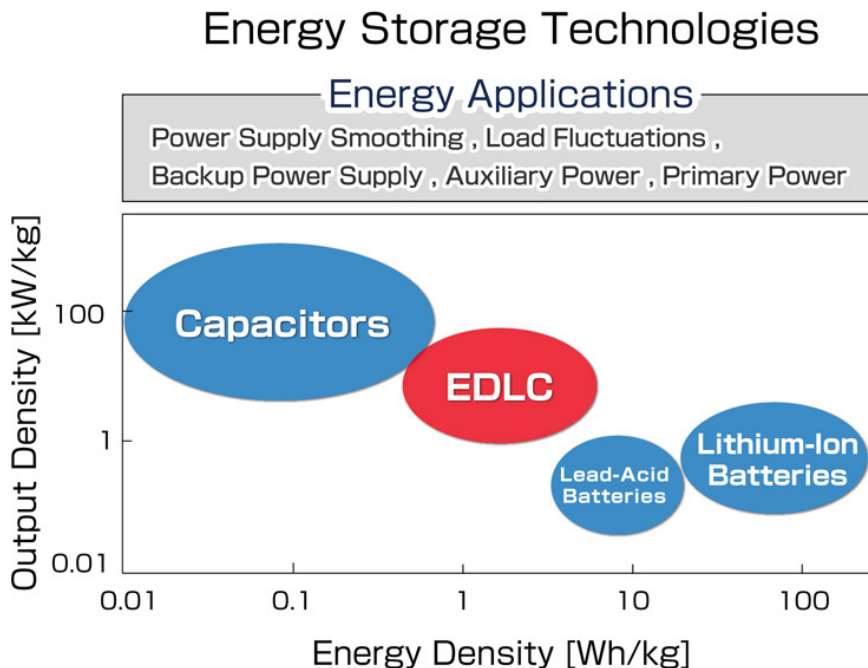
Energy Storage Technologies

Figure 1: Energy storage technology [28].

Supercapacitors can be divided into two types, based on the mechanism of the charge storage, pseudocapacitance and electric double layer capacitance (EDLC). In EDLC the charges are stored at the electrode electrolyte interface, while for pseudocapacitors the charges are generated within the electrode due to a faradic reaction. Therefore, electrochemical capacitors prepared using redox active materials exhibit higher specific capacitance than conventional EDLCs. Different types of transition metal oxides such as RuO_2, CuO, MnO_2, NiO, Co_3O_4, V_2O_5 have been shown a promise in pseudocapacitance [29-32]. For example ruthenium oxide (RuO_2) exhibits a high specific capacitance of 700 F g^{-1}, a wide potential window and reversible redox reactions [33,34].

Lee et al. reported high specific capacitance up to 1000 F g^{-1} based on the weight of hydrous RuO_2 [35]. However, the high cost of Ru based compounds limits the large-scale application in supercapacitor electrodes. Hence, much effort has been devoted to prepare a low cost alternative for RuO_2 that exhibits a high specific capacitance with a long cycle life. Nanostructured vanadium oxides have shown great promise for applications in energy storage. The redox-activity of vanadium oxides with multiple oxidation states (V^{+5}, V^{+4} and V^{+3}) is attractive for supercapacitors and Li ion batteries [36,37]. Moreover, V_2O_5 is a promising candidate for electrochemical capacitors due to the layered structure and ability to intercalate three Liþ ions per V_2O_5 unit yielding a theoretical capacitance of w400 mA h g^{-1} [38]. However, bulk V_2O_5 exhibits low electronic conductivity (10^{-2}-10^{-3} S cm^{-1}) and slow Li ion

diffusion rates (D w 10-12 cm^{-2} s^{-1}), leading to low initial capacitance and rapid capacitance fading [15]. In contrast, nanostructured vanadium oxides have shown improved Li ion diffusion rates [39]. To date, wide range of nanostructures such as nanotubes, nanowires, nanobelts and nanorods of V_2O_5 have been prepared [40-48]. Also, freestanding flexible papers of V_2O_5 nanowires (VNW) can be prepared by vacuum filtration. Unfortunately, due to the low electronic conductivity of the VNWs conducting materials such as carbon materials must be added. Liu et al. have prepared reduced graphene oxide (rGO) ~VNW composite electrodes for Li ion battery cathodes and exhibited promising performance for Li ion storage [49]. Rui and co-workers deposited polycrystalline V_2O_5 spheres on rGO sheets and demonstrated their high capacitance capabilities in Li ion batteries [50].
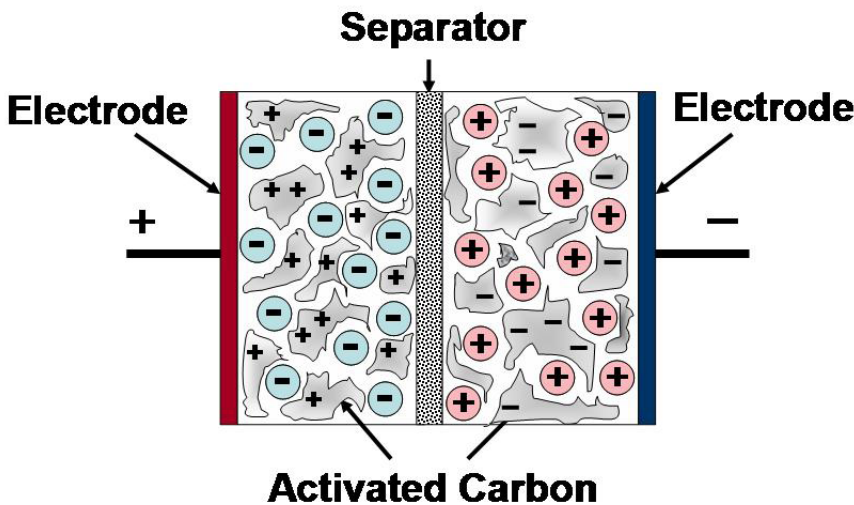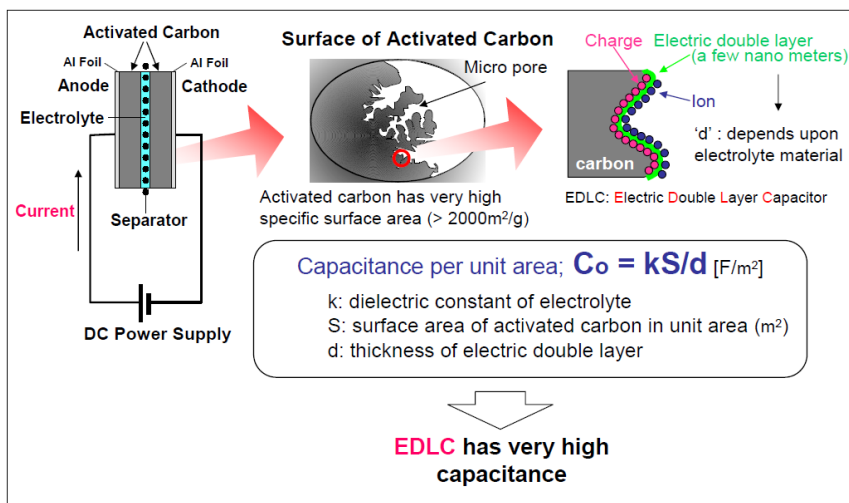

Figure 2: Basic principle of EDLC. [51]

Although significant efforts to enhance the supercapacitance of the transition metal oxide nanoparticles have been taken, the poor textural parameters of these electrodes make them less efficient. In addition, unsupported metal or metal oxide nanoparticles are generally not easy to handle and form aggregates under drastic conditions including oxidation and reduction. Therefore, researchers tried to decorate the redox metal oxides on supports with high surface areas in order to achieve high capacitance and good cycle life with the combined performance of EDLCs and pseudocapacitance [52,53]. Generally carbon supports with a high surface area are used for the redox metal oxide electrodes as they can store increased amount of energy on the high surface area porous structure. Recently, transition-metal-oxide-supported mesoporous materials have attracted attention as electrode materials. Some reports on the fabrication of transition-metal-oxide-supported mesoporous materials are available in the literature [54]. Of the various non-noble metals or transition-metal oxides studied, copper oxides are found to be very interesting because of its low cost, good thermal and electrical conductivity, and environmentally benign nature. Beyond these advantageous properties, copper oxide is very promising in a neutral electrolyte system. Recently, Vinu et al. reported the direct incorporation of a high amount of metal ions in the mesoporous SBA-15 silica framework by simply adjusting the water-to-hydrochloric acid molar ratio of the synthesis medium [55] without destroying the mesoporous structures. They also converted the copper substituted mesoporous silica into mesoporous carbon with the copper oxide nanoparticles and studied their performance for supercapacitors [56].

Many improvements have been made in the decades since Becker's precedent. Highly stable electrolyte systems, such as those based on non-aqueous solvents or ionic liquids, have allowed the operating potential of supercapacitor devices to be increased significantly, leading to higher energy and power densities compared to first generation, aqueous devices [57,58]. In addition to advances in electrolyte stability, advances have also been made in the carbon materials used as the electrodes. Examples include EDLCs containing electrodes comprised of carbon fabrics [59], fibers [60], nanotubes [61], nano-onions [62], aerogels [63], and graphene [57,58]. One common method for producing carbon materials is the pyrolysis of carbon containing polymers [64–66]. Applying pyrolysis techniques to powdered animal bones can produce a bone char containing a high percentage of conductive carbon with specific surface areas of approximately $2100 m^2/g$ [67,68]. These materials have been demonstrated to work as cathodes in lithium–sulfur batteries [68].

The objective of this paper is to review advances in flow field of materials, designs and electride performance of EDLCs, and analyze main issues and challenges in concepts and criteria of flow field in the development of application models. We focus on why uneven flow distribution is a root cause of low durability and reliability at the industrial scale and why flow field designs and electrical performance are a strategic solution to integrated performance, flow conditions, structure and electrochemical processes. Finally, we will discuss fundamental materials, characteristic parameters and procedures to tackle the challenges of uneven flow distribution during EDLC as well as critical issues of durability, robustness and reliability in the application field.

2. Materials and Performance

The attraction of carbon as a supercapacitor electrode material arises from a unique combination of chemical and physical properties, namely:

- high conductivity,
- high surface-area range (~1 to >2000m^2 g^{-1}),
- good corrosion resistance,
- high temperature stability,
- controlled pore structure,
- processability and compatibility in composite materials,
- relatively low cost.

In general terms, the first two of these properties are critical to the construction of supercapacitor electrodes. As will be seen, the properties of carbon allow both conductivity and surfacearea to be manipulated and optimised. Such activities continue to be the subject of a considerable amount of research. Prior to reviewing the results of this research, it is useful first to consider in more detail other aspects of carbon, e.g., its structural diversity and chemical behaviour, so as to establish a better understanding of the role of carbon materials in supercapacitors.

Table 2
Raw material costs and carbon yields from pyrolysis of some of the natural precursors [69,70].

Raw material	Raw material cost ($ kg^{-1})	Carbon yield from pyrolysis (wt.%)
Petroleum coke	1.4	90
Charcoal	1.2	90
Lignite	0.75	50
Coconut shell	0.25	30
Wood	0.8	25
Potato starch	1.0	45
Sucrose	0.25	<45
Cellulose	0.65	<45
Corn grain	0.25	<45
Banana fiber	4	<45

Activated carbons can be obtained by two different processes: the "physical" or "thermal" activation and the "chemical" activation. In the former carbonization is followed

by the activation of the resulting char at elevated temperature in the presence of suitable oxidizing gases such as carbon dioxide, steam, air or their mixtures; in the second one, carbonization and activation are performed in a single step, using a chemical agent [71] such as KOH, NaOH, H_3PO_4, $ZnCl_2$ etc. In comparison to physical activation, chemical activation provides two important advantages. One is the lower temperature at which the process is performed. The other is that the global yield of chemical activation tends to be greater because burn off char is not required [72]. Besides, part of the added chemicals (such as zinc salts and phosphoric acid), can be easily recovered. However, a two-step process (an admixed method of physical and chemical processes) can be applied.

Activated carbons exhibit low specfic surface areas when physical activation is applied due to its high silica content [73]. By physical activation with employing CO_2, steam or air, it is possible to obtain activated carbons with BET specific surface area (SBET) up to about 1180 m^2/g and pore volume up to about 1.09 cm^3/g [73-75]. In the case of chemical activation, where KOH/NaOH, K_2CO_3, $ZnCl_2$, H_3PO_4 as activating agents are usually being used, Chemical impregnation with KOH and NaOH of pyrolysed rice husks followed by activation at 650–800 °C resulted in activated carbons with extremely high surface areas (280–3014 m^2/g) and pore volume up to 1.88 cm^3/g [76-78]. Pyrolysis of rice husks followed by H_3PO_4 impregnation and activation at high temperatures (700–900 °C) produced activated carbon with a surface area of 420–438.9 m^2/g [78–80]. Generally use of other chemical agents, such as $ZnCl_2$, K_2CO_3/Na_2CO_3, $CaCl_2.7H_2O$ and H_2SO_4, and activation at 600–900 °C resulted in activated carbons with surface areas ranging from 66 to 1581 m^2/g, while the total pore volume and mean radius (d) are in the average ranges from 0.27 to 0.536 cm^3/g and 1.076 to 3.528 nm respectively [81-85].
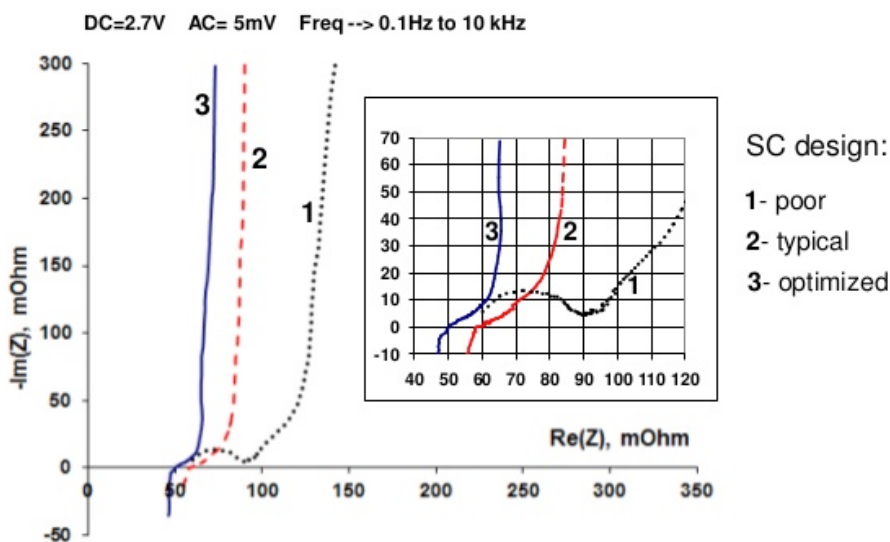

Figure 3: Nyquist plots for the activated carbon based EDLC. [86]

Activated carbon was prepared by placing firewood in a sealed oven reaching a temperature of 550°C in oxygen-deficient environment [87]. A carbonization process takes place. Steam was introduced in the oven at this temperature and the temperature was raised at 900°C. The resulted carbon was ground in a mill washed with pure water, dried, and sieved in granules with a size of 0.12–0.2 mm. Analysis indicated for such activated carbon micropores with a diameter lower than 2 nm and mesopores centered at 4 nm. Pores with a diameter lower than 2 nm are considered micropores, those with diameter in the range 2–50 nm, mesopores and those with diameter higher than 50 nm, macropores. Specific capacitance as high as 120 F/g was obtained from such activated material used in EDLC prepared electrodes and acidic solution. Petroleum needle coke was used in Ref. [88] for porous carbon preparation by means of KOH activation. The raw material was pulverized at size of 0.1–0.15mm and then mixed with KOH and placed in a stainless steel reactor at 750–900°C in argon environment for duration of 1–4 h. After washing in dilute HCl, pure water and drying, activated carbon resulted. Specific surface area in the range of 400–2900 m^2/g was obtained by different activation time but the specific capacitance for electrodes was not higher than 44 F/g. In Ref. [89] various coal and pitch derived carbonaceous materials were activated for 5 h at 800°C using KOH at 1:4 component ratio. For specific surface area in a range of 1900–3200 m^2/g specific capacitance from 200 to 320 F/g was obtained. Coal-based porous carbon activated by steam [90] exhibited mesopores with specific surface area of 340–1270 m^2/g. A maximum specific capacitance of 160 F/g was obtained. Specific capacitance of 79 F/g for activated carbon of 1660 m^2/g specific surface area, obtained from coconut shells was reported in Ref. [91]. Experiments on other fruit shell type [92] indicated lower specific capacitance. High specific capacitance of 294 F/g at current density of 1 mA/cm^2 for activated carbon resulted from resorcinol and formaldehyde is reported in Ref. [93]. These two substances catalyzed by KOH in a sol–gel process were carbonized in an inert atmosphere and KOH serves as activating agent producing pores. Increase in the proportion of KOH leads to higher specific surface area and pore volume. For porous carbon obtained from cresol-formaldehyde aerogel a specific capacitance of 146 F/g was reported [94]. In Ref. [95] it is shown that development of pore structures during KOH activation depends on the starting carbon material. The specific surface area increases as a function of KOH addition. Different treatments of the aluminum current collectors were performed in Refs. [96,97] to increase supercapacitor performance. Sol–gel deposit of conducting carbonaceous material provided better results. A specific capacitance of 100 F/g and sheet resistance of 0.8Ocm^2 in organic electrolyte was obtained. An optimization of the pore distribution in the activated carbon material can lead to higher capacitor performance [98]. Bigger pores provide good transport of ions throughout the porous carbon layer whereas the smaller pores generate a large interfacial area. Carbon materials with highly ordered porous structure, with micropores and mesopores were prepared using for example, mesoporous silica, as template [99,100]. Carbon precursor (propylene, sucrose or pitch) is introduced into the pores of the silica matrix. After the removal of silica by acid treatment, carbon material with organized porosity is recovered. Values of specific capacitance in aqueous electrolyte were limited to 200 F/g. Electrochemical capacitors based on activated carbon

powders of specific surface area of 870 and 2600 m²/g were prepared by using organic ionic electrolytes [101]. Specific capacitances of 45 and 180 F/g corresponding to the two different powders have been found. The specific capacitance densities were of 5.2 and 6.9 mF/cm². Treatment of the exposed surface of activated carbon material with a surfactant sodium oleate resulted in significant improvement of the specific capacitance [102,103]. This is attributable to improvement in wettability at the exposed pore surface resulting in higher usable surface area. Experiments in Ref. [104] with five samples of activated carbon with specific surface area in the range 563–2692 m²/g resulted in specific capacitance in the range 28–267 F/g at room temperature. Acidic and alkaline solution electrolytes have been used. Significant difference in the specific capacitance may appear for acidic or alkaline solution. The average pore diameter was of 1.4–2.8 nm. Again, proportionality between the exposed specific surface area and the manifested specific capacity has not been found.

AC fibers are popular materials for the electrode of EDLC because of their large SSA and high electrical conductivity. Kim et al. [105] developed CNFs with exposed graphite edges for use as the electrode material of ECs. Among various modifications of CNFs, the olygoaniline/CNF composite showed the largest capacitance of 149 F/g. The formation of ethynylaniline linkages to the edges of KOH-activated CNFs effectively preserved mesopores, and combines DL capacitance with pseudocapacitance. Recently, Xu et al. [106] prepared AC fiber cloth electrodes with high DL capacitance and good rate capability from polyacrylonitrile fabrics by CO_2 activation. Although the SSA of the microporous AC fiber cloths is only between 527 and 834 m²/g, their specific capacitance in 6 mol/L KOH aqueous solution is over 168 F/g (carbonization temperature 900°C), and a moderate carbonization temperature (600°C) results in higher specific capacitance (208 F/g) recorded at 36 mA/cm².

ACF cloth electrodes for electrochemical capacitors were prepared from polyacrylonitrile (PAN) fabrics by optimization of the carbonization temperature prior to CO_2 activation [107]. A specific capacitance of 208 F/g was found at low current load. At 10 A/g a decrease to 129 F/g takes place. It is shown that template mesoporous carbons can provide 0.14 F/m² in aqueous electrolytes (example H_2SO_4 and KOH) and 0.06 F/m² in organic electrolyte [108]. For such material effective surface area as high as 1500–1600 m²/g is exhibited and the specific capacitance can reach 200–220 F/g in aqueous electrolyte and 100 F/g in organic electrolyte. Specific capacitance of 290 F/g for PAN-based carbon fibers used in electrodes for electrochemical capacitors is reported in Ref. [109]. H_2SO_4 as electrolyte solution was used. The specific surface area was 1300 m²/g. Microstructure and electric conductivity of PAN-based ACFs were investigated using tension and KOH activation [110]. Increase of KOH concentration caused damage to the surface of carbon fibers leading to higher specific surface. Increase in the micropore volume for PAN-based ACFs caused lower specific capacitance [111].

Recently, the CNTs have attracted much attention as new materials due to their good mechanical strength, high electric conductivity, and reasonable SSA since their first discovery by Katakabe et al. [112]. Honda's group [113] prepare a vertically aligned multi-walled carbon nanotube (MWCNT) sheet by a transfer procedure from a silicon substrate,

covered with catalyst grains as a CNT seedbed, with Al sheet as a current collector for the application of an EDLC. It is noteworthy that the MWCNT sheet electrode provides a discharge capacity of 10–15 F/g even at an extremely high current density (200 A/g), whereas no discharge capacitance is obtained at all with a typical high performance AC electrode at such a high current density. Recently, Show et al. [114] fabricated an EDLC with polarizable electrodes containing the CNTs. This EDLC shows a low equivalent series resistance of 2.5 U, which was lower than that of an EDLC fabricated with the addition of acetylene black. The low series resistance increased the energy and efficiency of the EDLC, because the IR drop, caused by flowing current according to the series resistance, is of a low value. Furthermore, the effect of pore size on the EDLC was studied by Ref. [115], the results showed that narrow pores was important to the EDLCs which had high energy density for longer discharge time, such as hybrid electric vehicles. But for pulse power applications, increasing the pore size might be beneficial.

Table 3
Summary of the various classes of electrode materials investigated. [116]

	Electrode material	Electrolyte	Working voltage (V)	Specific capacitance (F/g)
Carbon-based	Activated carbon (AC) [52]	1 M $Et_4NBF_4 + PC$	1.5	40
	Graphite [45]	1 M $Et_4NBF_4 + PC$	3.0	12
	Carbon aerogels (CAGs) [42]	1.5 M $Et_3MeNBF_4 + PC$	3.0	160
	Mesoporous carbon [20]	30 wt% KOH	0.9	180
	Meso/macroporous carbon [53]	6 M KOH	0.8	130
	C_{60}-loaded AC fibe [19]	0.5 mol/L H_2SO_4	1.0	172
	AC fiber cloth [47]	6 mol/L KOH	1.0	208
	Single-walled CNTs [22]	EMITFSI	2.3	50
	Multi-walled CNTs sheet [12]	1.96 M $TEMABF_4 + PC$	2.5	13
	CNTs/polypyrrole (PPy)/MnO_2 [49]	1.0 M Na_2SO_4	0.9	281

An electrode with vertically aligned multiwalled carbon nanotubes [117], provided a discharge capacity of 10–15 F/g even at an extremely high current density of 200 A/g. It is said that such performance is not possible with activated carbon electrode. For CNT electrodes used in Ref. [118] a specific capacitance of 14 F/g is mentioned. In Refs. [119,120] addition of CNTs to activated carbon, instead of acetylene black or graphite powder for polarizable electrodes resulted in lower ESR and higher specific capacitance. Addition of CNTs in activated carbon material [121] increased specific capacitance from 130 to 180 F/g. Supercapacitor electrodes prepared from CNTs/ ruthenium oxide composite exhibited significantly higher specific capacitance due to a pseudocapacitance originated from the RuO_2 nanoparticles [122–126]. In Ref. [127] $Ni(OH)_2$/MWCNT composite positive electrodes and activated carbon negative electrodes delivered a specific energy of 32 Wh/kg at a specific power of 1500 W/kg based on the total weight of the active electrode materials. This was possible by significant increase in the specific capacitance. In Ref. [128] nickel oxide/CNTs composite electrode resulted in an increased specific capacitance of 52 F/g. In Ref. [129] nonaqueous hybrid supercapacitor using manganese oxide/MWCNTs (M/M) composite

and MWCNTs as positive and negative electrodes, respectively, has been designed and investigated by constant current charge/discharge tests. The asymmetric hybrid capacitor has better capacitance and energy characteristics than those of the symmetric ones based on individual M/M composite and MWCNTs electrodes. The energy density of the hybrid capacitor can reach 32.91 Wh/kg even at a current density of 10 mA/cm^2 in 1.0M LiClO$_4$ electrolyte, which is comparable to that of a manganese oxide/activated carbon hybrid capacitor. Manganese oxide/CNT nanocomposite electrodes used in supercapacitors [130–133] resulted in better performance than CNTs electrodes. An increase of specific capacitance takes place. SWCNTs/polypyrrole nanocomposite electrode used in Refs. [134,135] indicated much higher specific capacitance than pure polypyrrole or SWCNTs electrodes. Supercapacitor electrodes based on carbon nanotube–polyaniline (CNT–PANI) nanocomposite by coating polyaniline on the surface of the CNT have been used in Ref. [136]. At a current density of 10 mA/cm, the CNT–PANI nanocomposite exhibits high specific capacitance of 201 F/g, in comparison with a value of 52 F/g for the CNT. The supercapacitors based on the CNT–PANI nanocomposite have an energy density of 6.97 Wh/kg and an outstanding power performance. Composite materials containing 20wt% of MWCNTs and 80wt% of chemically formed conducting polymers as polyaniline and polypyrrole have been prepared and used for supercapacitor electrodes in Ref. [137].
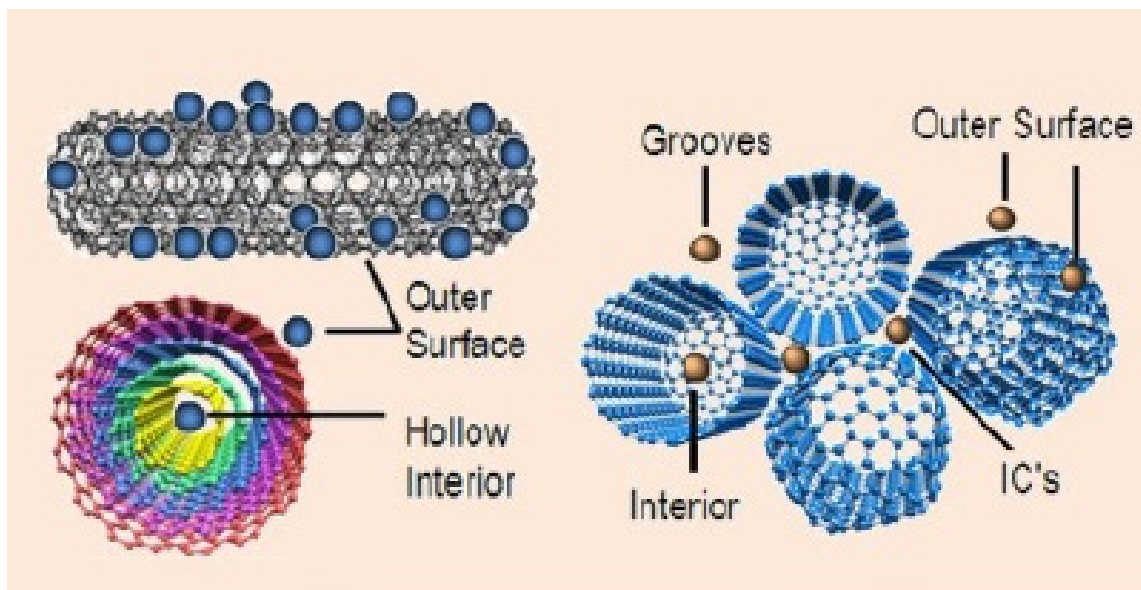

Figure 4: Possible binding sites available for adsorption on (left) MWNTs and (right) SWNTs surfaces [138].
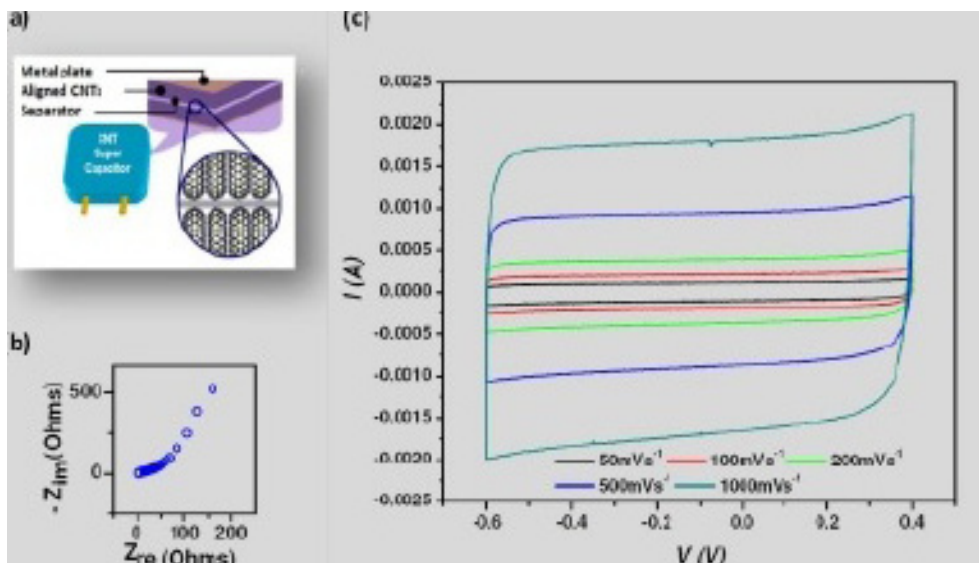
Figure 5: (a) Artist rendition of EDLC formed by aligned MWNT grown directly on metals (b) An electrochemical impedance spectroscopy plot showing low ESR of such EDLC devices and (c) very symmetric and near rectangular cyclic voltamograms of such devices indicating impressive capacitance behavior. [138]
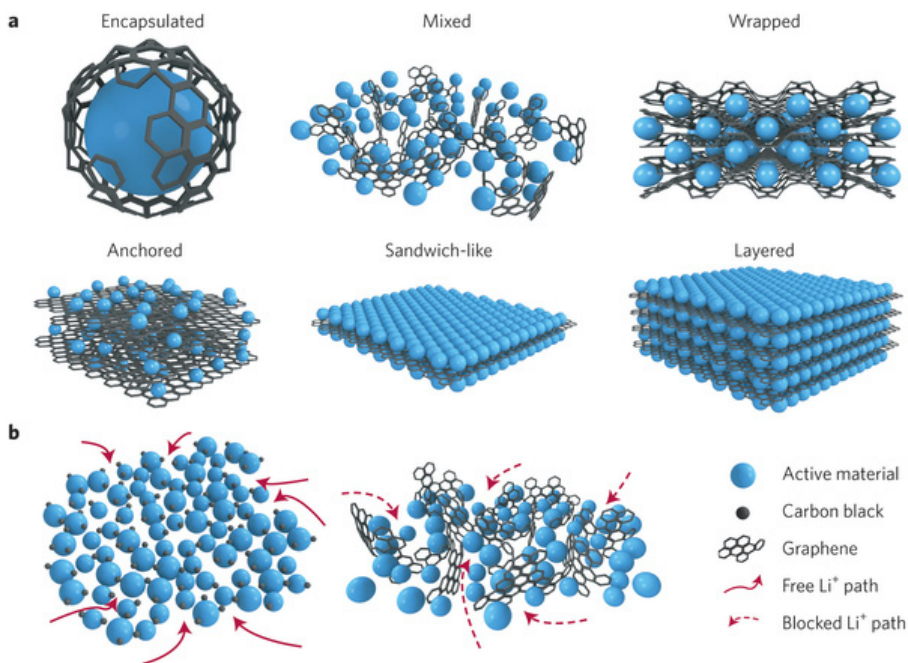

Figure 6: The role of graphene for electrochemical energy storage [139].

The capacitive behavior of graphene sheets can be further improved by chemical doping or etching, both the presence of electro-active species and surface area of the pores can contribute to the total specific capacitance. For example, N-doped graphene hydrogels (NGHs) prepared by a solvothermalmethod displayed a specific capacitance of 205 F g^{-1} at scan rate of 1.0 mV s^{-1} [139]. After 3000 cycle tests at a scan rate of 80 mVs^{-1}, about 92.6% of the capacitancewas preserved. Furthermore, an energy density of 3.65Wh $kg^{-1}$was exhibitedwhen a power density of 20.5 kW kg^{-1} was achieved at discharging current density of 100 A g^{-1}. Using hydrothermal process, Chen et al. synthesized a NGH using organic amine and GO as precursor and the prepared hydrogels were immersed in KOH aqueous before the electrochemical measurement [140]. The supercapacitors exhibited a power density of 205.0 kW kg^{-1} at a charge/discharge rate of 185.0 A g^{-1} and a specific capacitance of 113.8 F g^{-1} with good cycling stability (95.2% of capacitance was retained after 4000 cycles). There are two reasons for these remarkable performances: (i) a larger binding energy of the basal-plane pyridinic N and pyrrolicNresults in a larger number of ions to be accommodated on the electrode surface; (ii) big porous network and flat graphene structure contribute to fast adsorption and diffusion of potassium ion on electrode surface, leading to a fast charge/discharge rate and a very high power density. Incorporating "stabilizer" or "spacer" into 3D graphene architectures is one of the most promising ways to improve supercapacitors performance, especial in using pseudo-active materials, such as metal [141], metal oxides 142,143,144,145,146, 147,148–150,151,152–154, 155–162], conductive polymers [163,164,165,166,167,168–174] and carbon nanotubes [175]. For example, 3D graphene/Ni(OH)$_2$ composite hydrogels prepared by Xu and coworkers exhibited a specific capacitance of ~1212 F g^{-1} at a discharge rate of 2 A g^{-1}, while only ~309 F g^{-1} for the physical mixture of these two components was obtained [143]. After the cycling test at 16 A g^{-1} for 2000 charge and discharge cycles, only a slight decrease in capacitance (~5%) was exhibited. Similarly, using 3D hierarchical β-Ni(OH)$_2$ hollow microspheres wrapped in rGO, Wang et al. [176] obtained a specific capacitance of 1551.8 F g^{-1} at a current density of 2.67 A g^{-1} and a capacity retention of 102% after 2000 cycles. The good performance of these composites mainly results in the synergetic effect of graphene and the other components. First, the pseudo-capacitive materials contribute pseudocapacitance to the whole composite electrode. Second, graphene sheets can effectively prevent the aggregation of nanoparticles and make full use of the electrochemically active material. Third, the interconnected porous 3D structure facilitates electrolyte diffusion as well as electron transport through electrically conductive channel. Tour et al. fabricated a supercapacitor based on seamless three-dimensional carbon nanotube and graphene hybrid material [175].
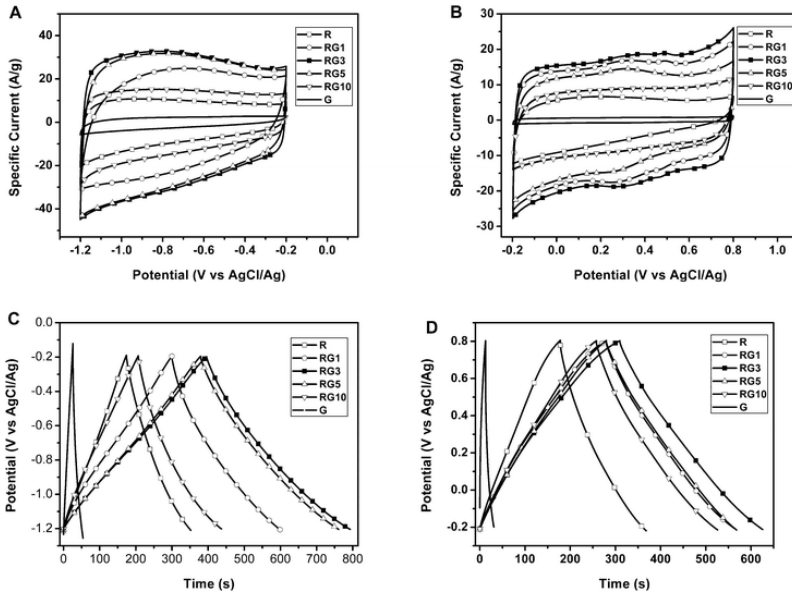
Figure 7: Pyrolyzed graphene oxide/resorcinol-formaldehyde resin composites as high-performance supercapacitor electrodes [177]
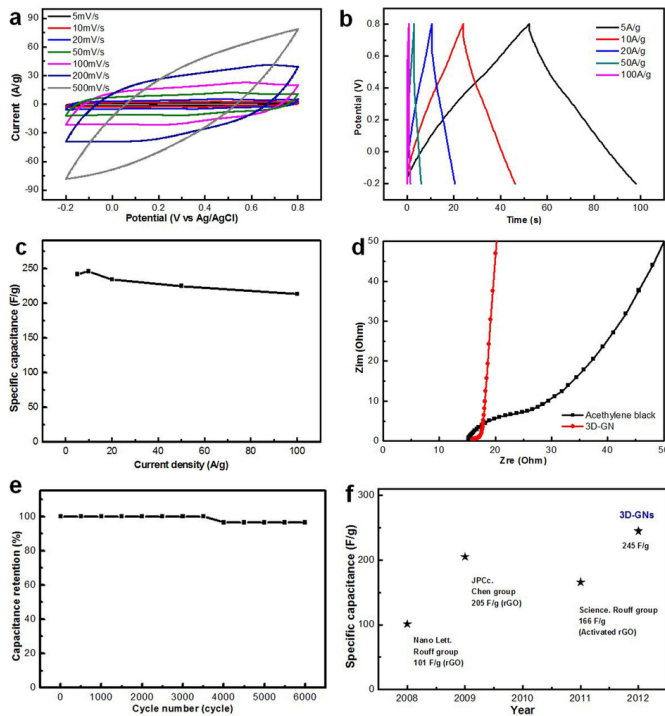

Figure 8: Electrochemical performance of 3D-GN-based supercapacitor. [178]

3. Conclusion

We summarized the progress to date on the electrode materials of ECs, including carbon-based materials. Based on previous reports, the key factors that dictate the selection of electrode materials for ECs are the following: (1) high SSA, leading to the large capacitance; (2) suitable surface functional groups to enhance the capacitance by additional faradaic redox reaction and improve the wettability; (3) large pore size, short pore length, and straightforward pore connectivity to facilitate the ions diffusion with a high speed; (4) low internal electric resistance, which leads to fast charging-discharging and low ohmic resistance; (5) low volume and weight; (6) low price; (7) environmentally friendly materials; (8) thinner electrodes and current collectors. carbon-based materials with macro-, micro- and nano-structures have been applied to construct various attractive electrochemistry energy devices, sorbents and catalysts. A variety of methods including hydrothermal/solvothermal reaction, self-assembly, organic sol–gel reaction and template guided growth have been developed for preparing carbon based materials. Especially, the 3D architectures do not only assemble graphene nanosheets into macroscopic materials for practical applications but also provide fundamental frame works with more "space" for loading inorganic nanoparticles, organic or biological molecules. Although extensive efforts have been devoted, studies about materials fabrication and their applications in energy and environmental-related field are still in primary stages. At least, the following challenges still remain. A green and facile method is highly required to synthesize 3D graphene architectures with designed compositions, shapes, pore sizes and porosity. For instance, large pores with size up to a few hundred nanometers in 3D graphene framework are not good for electrolyte filtration in supercapacitors, resulting in low electric double layer capacitance. To enhance the capacitance (or energy density) of pure 3D graphene, pseudo-capacitive materials are usually suitable. Among the numerous potential dopants, what are the most suitable and efficient dopants and methods for the improved capacitive behavior of 3D graphene materials? So there is tremendous room available in the design and synthesis of novel carbon-based materials for energy-related applications. Although some literatures indicated that carbon-based materials products have prominent ability in the field of pollutants detection and environmental remediation. There are a lot of pollutants and microorganism that exist in circumstance, and only a small part of them have been explored. Thus, the mechanisms of pollutants detection and removal based on multifunctional carbon-based materials need to be further developed. Porous carbon-based materials with the porosity and flow characteristics can be applied for flow-through reactors in separation and catalytic processes. The safe operation and "green chemistry" in environmental protection should also be considered for practical applications.

References

[1]   S.G. Kandalkar, H.M. Lee, S.H. Seo, K. Lee, C.K. Kim, *Korean J. Chem. Eng*. 28 (6) (2011) 1464.

[2]   S. Mitani, S. I. Lee, K. Saito, Y. Korai, I. Mochida, *Electrochim. Acta* 51 (2006) 5487.

[3]   M.F. E. Kady, V. Strong, S. Dubin, R.B. Kaner, *Science* 335 (2012) 1326.

[4]   L. Wei, G. Yushin, *Nano Energy* 1 (2012) 552.

[5]   P. Sharma, T.S. Bhatti, *Energy Convers. Manage*. 51 (2010) 2901.

[6]   B.E. Conway, *Kluwer Academic/Plenum*, New York, 1999.

[7]   R. Kotz, M. Carlen, *Electrochim. Acta* 45 (2000) 2483.

[8]   M. Conte, *Fuel Cells* 10 (2010) 806.

[9]   Y. Zhang, H. Feng, X.B. Wu, L.Z. Wang, A.Q. Zhang, T.C. Xia, H.C. Dong, X.F. Li, L.S. Zhang, *Int. J. Hydrogen Energy* 34 (2009) 4889.

[10] R.B. Rakhi, W. Chen, H.N. Alshareef, *J. Mater. Chem*. 22 (2012) 5177.

[11] M. Inagaki, H. Konno, O. Tanaike, *J. Power Sources* 195 (2010) 7880.

[12] A.G. Pandolfo, A.F. Hollenkamp, *J. Power Sources* 157 (2006) 11.

[13] G.M. Jacob, Q.M. Yang, I. Zhitomirsky, *J.Appl. Electrochem*. 39 (2009) 2579.

[14] E. Jeonga, M. J. Jung, S.H. Cho, S.I. Lee, Y. S. Lee, *Colloids Surf., A* 377 (2011) 243.

[15] A. Elmouwahidi, Z. Z.Benabithe, F. C. Marin, C. M. Castilla, *Bioresour. Technol.* 111 (2012) 185.

[16] C.C. Liu, D.S. Tsai, W.H. Chung, K.W. Li, K.Y. Lee, Y.S. Huang, *J. Power Sources* 196 (2011) 5761.

[17] H. Wang, C. Peng, F. Peng, H. Yu, J. Yang, *Mater. Sci. Eng*., B 176 (2011) 1073.

[18] C. Yuan, L.Hou, Y. Feng, S. Xiong, X. Zhang, *Electrochim. Acta* 88 (2013) 507.

[19] E. Frackowiak, S. Delpeux, K. Jurewicz, K. Szostak, D. Cazorla-Amoros, F. Béguin, *Chem. Phys. Lett.* 361 (2002) 35.

[20] H. Kim, N.J. Jeong, S.J. Lee, K.S. Song, Korean *J. Chem. Eng*. 25 (3) (2008) 443.

[21] Y.J. Lee, J.C. Jung, J. Yi, S.-H. Baeck, J.R. Yoon, I.K. Song, *Curr. Appl. Phys*. 10 (2010) 682.

[22] Z. Zapata-Benabithe, F. Carrasco-Marín, C. Moreno-Castilla, *Mater. Chem. Phys*. 138 (2013) 870.

[23] H.W. Park, U.G. Hong, Y.J. Lee, I.K. Song, *Appl. Catal., A: Gen.* 409e410 (2011) 167.

[24] B. Fang, L. Binder, *Electrochim. Acta* 52 (2007) 6916.

[25] B. Fang, L. Binder, *J. Power Sources* 163 (2006) 616.

[26] M. Molina-Sabio, F. Rodríguez-Reinoso, *Colloids Surf.,* A 241 (2004) 15.

[27] A.B. Fuertes, G. Lota, T.A. Centenob, E. Frackowiak, *Electrochim. Acta* 50 (2005) 2799-2805.

[28] https://www.google.co.kr/search?q=edlc&newwindow=1&biw=1273&bih=625&tbm=isch&tbo= u&source=univ&sa=X&sqi=2&ved=0CCsQsARqFQoTCJPs7AmccCFaPapgodVjwHmg &dpr=1#newwindow=1&tbm=isch&q=edlc+performance&imgrc=6UhKpKD3l9yVxM%3A.

[29] H. Wang, Y. Liang, T. Mirfakhrai, Z. Chen, H. Casalongue, H. Dai, *Nano Res*. 4 (2011) 729.

[30] J. Shaikh, R. Pawar, R. Devan, Y. Ma, P. Salvi, S. Kolekar, P. Patil, *Electrochim. Acta* 56 (2011) 2127.

[31] S. Chen, J. Zhu, X. Wu, Q. Han, X. Wang, *ACS Nano* 4 (2010) 2822.

[32] Y. Gao, S. Chen, D. Cao, G. Wang, J. Yin, *J. Power Sources* 195 (2010) 1757.

[33] J.P. Zheng, P.J. Cygan, T.R. Jow, *J. Electrochem. Soc*. 142 (1995) 2699.

[34] M. Min, K. MacHida, J. Jang, K. Naoi, *J. Electrochem. Soc.* 153 (2006) A334.

[35] B.J. Lee, S. Sivakkumar, J.M. Ko, J.H. Kim, S.M. Jo, D.Y. Kim, *J. Power Sources* 168 (2007) 546.

[36] S. Boukhalfa, K. Evanoff, G. Yushin, *Energy Environ. Sci.* 5 (2012) 6872.

[37] D. Choi, G. Blomgren, P. Kumta, *Adv. Mater*. 18 (2006) 1178.

[38] Z. LI, J. Tang, J. Yang, C. Cheng, Q. Xiao, G. Lei, *Funct. Mater. Lett*. 4 (2011) 61.

[39] Y.L. Cheah, N. Gupta, S.S. Pramana, V. Aravindan, G. Wee, M. Srinivasan, *J. Power Sources* 196 (2011) 6465.

[40] S.D. Perera, B. Patel, N. Nijem, K. Roodenko, O. Seitz, J.P. Ferraris, Y.J. Chabal, K.J. Balkus, *Adv. Energy Mater*. 1 (2011) 936.

[41] M. Roppolo, C. Jacobs, S. Upreti, N. Chernova, M. Whittingham, *J. Mater. Sci.* 43 (2008) 4742.

[42] S.D. Perera, B. Patel, J. Bonso, M. Grunewald, J.P. Ferraris, K.J. Balkus, *ACS Appl. Mater. Interfaces* 3 (2011) 4512.

[43] W. C. Fang, W.L. Fang, *Chem. Commun*. 41 (2008) 5236.

[44] Z. Chen, Y. Qin, D. Weng, Q. Xiao, Y. Peng, X. Wang, H. Li, F. Wei, Y. Lu, *Adv. Funct. Mater*. 19 (2009) 3420.

[45] C. Xiong, A.E. Aliev, B. Gnade, K.J. Balkus, *ACS Nano* 2 (2008) 293.

[46] Y. Wang, H. Zhang, W. Lim, J. Lin, C. Wong, *J. Mater. Chem*. 21 (2011) 2362.

[47] K. Takahashi, Y. Wang, G. Cao, *Appl. Phys. Lett*. 86 (2005) 1.

[48] G. Wee, H.Z. Soh, Y.L. Cheah, S.G. Mhaisalkar, M. Srinivasan, *J. Mater. Chem*. 20 (2010) 6720.

[49] H. Liu, W. Yang, *Energy Environ. Sci.* 4 (2011) 4000.

[50] X. Rui, J. Zhu, D. Sim, C. Xu, Y. Zeng, H.H. Hng, T.M. Lim, Q. Yan, Nanoscale 3 (2011) 4752.

[51] https://www.google.co.kr/search?q=edlc&newwindow=1&biw=1273&bih=625&tbm=isch&tbo=u&source=univ&sa=X&sqi=2&ved=0CCsQsARqFQoTCJPsd7AmccFaPapgodVjwHmg&dpr=1#imgrc=-DSxwG-IueOenM%3A.

[52] R.A. Catalao, F.J. Maldonado-Hodar, A. Fernandes, C. Henriques, M.F. Ribeiro, *Appl. Catal.* B 88 (2009) 135.

[53] H. Yamashita, H. Yamada, A. Tomita, Appl. Catal. 78 (1991) L1. [27] H. Huwe, M. Froba, <u>Carbon </u>45 (2007) 304.

[54] N.A. Fellenz, S.G. Marchetti, J.F. Bengoa, R.C. Mercader, S.J. Stewart, *J. Magn. Magn. Mater.* 306 (2007) 30.

[55] A. Vinu, V. Murugesan, W. Bohlmann, M. Hartmann, *J. Phys. Chem.* B 108 (2004) 11496.

[56] K.P.S. Prasad, D.S. Dhawale, T. Sivakumar, S.S. Aldeyab, J.S.M. Zaidi, K. Ariga, A. Vinu, *Sci. Technol. Adv. Mater.* 12 (2012) 044602.

[57] M.D. Stoller, S. Park, Y. Zhu, J. An, R.S. Ruoff, *Nano. Lett*. 8 (2008) 3498.

[58] S.R.C. Vivekchand, C.S. Rout, K.S. Subrahmanyam, A. Govindaraj, CNR Rao. *J. Chem. Sci*. 120 (2008) 9.

[59] K. Hung, C. Masarapu, T. Ko, B .Wei, *J. Power. Sour*. 193 (2009) 944.

[60] J.H. Lin, T.H. Ko, Y.H. Lin, C.K. Pan, *Energy. Fuels.* 23 (2009) 4668.

[61] F. Pico, J.M. Rojo, A. Anson, A.M. Benito, M.A. Callejas, *J. Electrochem. Soc*. A 151 (2004)831.

[62] E.G. Bushueva, P.S. Galkin, A.V. Okotrub, L.G. Bulusheva, N.N. Gavrilov, V.L. Kuznetsov, *Phys Status. Solidi.* B 245 (2008) 2296.

[63] R.Saliger, U. Fischer, C. Herta, J. Fricke, *J. Non-Cryst. Solids*. 225 (1998) 81.

[64] S.S. Barton, M.J.B. Evans, B.H. Harrison, J. Colloid. *Interface. Sci*. 49 (1974) 462.

[65] S. Korkut, J.D. Roy-Mayhew, D.M. Dabbs, D.L. Milius, I.A. Aksay, *ACS Nano*. 5 (2011) 5214.

[66] Y. Tao, M. Endo, M. Inagaki, K. Kaneko, *J. Mater. Chem*. 21 (2011) 313.

[67] B. Purevsuren, B. Avid, J. Narangerel, T. Gerelmaa, Y. Davaajav, J. *Mater. Sci*. 39 (2004) 737.

[68] S. Wei, H .Zhang, Y. Huang, W. Wang, Y. Xia, Z. Yu, *Energy Environ Sci* 4 (2011) 736.

[69] G.G. Stavropoulos, A.A. Zabaniotou, *Fuel. Process. Technol*. 90 (2009) 952.

[70] L. Wei, G. Yushin, *Carbon* 49 (2011) 4830.

[71] M.N. Norhusna, L.C.Lau, K.T.Lee, R.M.Abdul, *J. Environ. Chem. Eng.* 1 (2013) 658.

[72] K. Mohanty, J.T. Naidu, B.C. Meikap, M.N. Biswas, *Ind. Eng. Chem. Res*. 45 (2006) 5165.

[73] C. Deiana, D. Granados, R. Venturini, A. Amaya, M. Sergio, N. Tancredi, *Ind. Eng. Chem. Res* 47 (2008) 4754.

[74] S. Kumagai, K. Sasaki, Y. Shimizu, K. Takeda, *Sep. Purif. Technol*. 61 (2008) 398.

[75] S. Kumagai, Y .Shimizu, Y. Toida, Y. Enda, *Fuel*. 88 (2009) 1975.

[76] J.C.C Freitas, M.A. Schettino, A.G. Cunha, F.G. Emmerich, A.C. Bloise, E.R. Azevedo, *Carbon*. 45 (2007) 1097.

[77] A.A.M. Daifullah, B.S. Girgis, H.M. Gad. *Mater. Lett*. 57 (2003) 1723.

[78] I.A. Rahman, B. Saad, S. Shaidan, E.S. Rizal. Bioresour. *Technol*. 96 (2005) 1578.

[79] L.J. Kennedy, J.J. Vijaya, G. Sekaran. *Ind. Eng. Chem. Res*. 4 (2004) 1832.

[80] L.J. Kennedy, K. Mohan, G. Sekaran, *Carbon*. 42 (2004) 2399.

[81] D. Kalderis, S. Bethanis, P. Paraskeva, E. Diamadopoulos, *Bioresour. Technol*. 99 (2008) 6809.

[82] P.M. Yeletsky, V.A. Yakovlev, M.S. Melgunov, V.N. Parmon, *Micropor. Mesopor. Mat*. 121 (2009) 34.

[83] E.I., E.l.Shafey. J. Hazard. *Mater*. 147 (2007) 546.

[84] P. Mondal, C.B. Majumder, B Mohanty. *Ind. Eng. Chem. Res*. 46 (2007) 2550.

[85] D. Mohan, K.P. Singh, V.K. Singh, *J. Hazard. Mater*. 152 (2008) 1045.

[86] https://www.google.co.kr/search?q=edlc&newwindow=1&biw=1273&bih=625&tbm=isch&t bo= u&source=univ&sa=X&sqi=2&ved=0CCsQsARqFQoTCJPs7AmccCFaPapgodVjwHmg &dpr=1#newwindow=1&tbm=isch&q=edlc+performance&imgrc=n6QFGFJrJVjsjM%3A.

[87] W.M. Qiao, S.H. Yoon, I. Mochida, *Energy Fuels* 20 (2006) 1680.

[88] K. Kierzek, et al., *Electrochim. Acta* 49 (2004) 515.

[89] G. Gryglewicz, *Electrochim. Acta* 50 (2005) 1197.

[90] P.W. Zhou, et al., *New. Carbon. Mater*. 21 (2006) 125.

[91] C.C. Hua, C.C. Wang, F.C. Wu, R.L. Tseng, *Electrochim. Acta* 52 (2007) 2498.

[92] Y. Zhu, H. Hu, W. Li, X. Zhang, *Carbon*. 45 (2007) 160.

[93] Y. Zhu, H. Hu, W.C. Li, X. Zhang, *J. Power. Sources*. 162 (2006) 738.

[94] Y.J. Kim, et al., *Carbon* 42 (12/13) (2004) 2423.

[95] C. Portet, P.L. Taberna, P. Simon, C. Laberty-Robert, *Electrochim. Acta* 49 (6) (2004) 905.

[96] C. Portet, et al., *J. Electrochem. Soc.* 153 (4) (2006) A649.

[97] M. Eikerling, A.A. Kornyshev, E. Lustd, *J. Electrochem. Soc.* 152 (1) (2005) E24.

[98] C. Vix-Guterl, *Adv. Technol.* B 108 (2004) 148.

[99] C. Vix-Guterl, *Carbon*. 43 (6) (2005) 1293.

[100] A. Lewandowski, M. Galiski, *J. Phys. Chem. Solids* 65 (2/3) (2004) 281.

[101] B. Fang, Y.Z. Wei, K. Suzuki, M. Kumagai, *Electrochim. Acta* 50 (18) (2005) 3616.

[102] B. Fang, Y.Z. Wei, M. Kumagai, *J. Power. Sour.* 155 (2) (2006) 712.

[103] B. Fang, L. Binder, *J. Power Sources* 163 (2006) 616.

[104] M. Toupin, D. Be´langer, I.R. Hill, D. *Quinn, J. Power. Sour.* 140 (1) (2005) 203.

[105] S.U. Kim, K.H. Lee, *Chem. Phys. Lett*. 400 (2004) 253.

[106] B Xu, F Wu, S Chen, C Zhang, G Cao, Y Yang, *Electrochim. Acta*. 52 (2007) 4595.

[107] B. Xu, et al., *Electrochim. Acta*. 52 (13) (2007) 4595.

[108] M. Sevilla, et al., *Electrochim. Acta* 52 (9) (2007) 3207.

[109] K.P. Wang, H. Teng, *Carbon* 44 (2006) 3218.

[110] J.G. Lee, J.Y. Kim, S.H. Kim, *J. Mater. Sci*. 42 (2007) 2486.

[111] J.G. Lee, J.Y. Kima, S.H. Kim, *J. Power. Sources*. 160 (2006) 1495.

[112] T. Katakabe, T. Kaneko, M. Watanabe, T. Fukushima, T. Aida, *J. Electrochem. Soc*. 152 (2005) 1913–6.

[113] Y. Honda, T. Haramoto, M. Takeshige, H. Shiozaki, T. Kitamura, M. Ishikawa, Electrochem. *Solid-State. Lett*. 10 (2007) 106.

[114] Y. Show, K. Imaizumi, D. Relat, *Mater*. 16 (2007) 1154.

[115] J. Chmiola, G. Yushin, Y. Gogotsi, C. Portet, P. Simon, P.L. Taberna, *Science*, 313 (2006) 1760.

[116] Y. Zhang, H. Feng, X.B. Wu, L.Z. Wang, A.Q. Zhang, T.C. Xia, H.C. Dong, X.F. Li, L.S. Zhang, *Inter. J. Hydro. Ener*. 34 (2009) 4889.

[117] Y. Honda, et al., *Electrochem. Solid State Lett*. 10 (4) (2007) A106.

[118] D. Tashima, *Thin Solid Films* 515 (9) (2007) 4234.

[119] Y. Show, K. Imaizumi, *Diamond Relat. Mater.* 15 (11/12) (2006) 2086.

[120] C. Portet, P.L. Taberna, P. Simon, E. Flahaut, *J. Power Sources* 139 (2005) 371.

[121] C.G. Liu, et al., *New Carbon Mater*. 20 (3) (2005) 205.

[122] X.F. Wang, D.Z. Wang, D. Liang, *Acta. Phys.Chim. Sin*. 19 (6) (2003) 509.

[123] Y.T. Kim, K. Tadai, T. Mitani, *J. Mater. Chem*. 15 (46) (2005) 4914.

[124] J.K. Lee, H.M. Pathan, K.D. Jung, O.S. Joo, *J. Power Sources* 159 (2006) 1527.

[125] X.F. Wang, Q. Gao, J. Liang, *Rare Metal Mater. Eng*. 35 (2) (2006) 295.

[126] Z.Y. Sun, et al., *Carbon* 44 (2006) 888.

[127] Y.G. Wang, L. Yu, Y.Y. Xia, *J. Electrochem. Soc*. 153 (4) (2006) 743.

[128] X.F. Wang, D.Z. Wang, L. Liang, *J. Inorg. Mater*. 18 (2) (2003) 331.

[129] G.X. Wang, B.L. Zhang, Z.L. Yu, M.Z. *Qu, Solid State Ionics* 176 (11/12) (2005) 1169.

[130] C.Y. Lee, et al., *J. Electrochem. Soc*. 152 (4) (2005) A716.

[131] E. Raymundo-Pinero, V. Khomenko, E. Frackowiak, F. Beguin, *J. Electrochem. Soc*. 152 (1) (2005) A229.

[132] V. Subramanian, H. Zhu, B. Wei, *Electrochem. Commun.* 8 (2006) 827.

[133] Z. Fan, et al., *Diamond Relat. Mater*. 15 (2006) 1478.

[134] K.H. An, et al., *J. Electrochem. Soc.* 149 (8) (2002) A1058.

[135] H.T. Ham, Y.S. Choi, N. Jeong, I.J. Chung, *Polymer* 46 (2005) 6308.

[136] M.G. Deng, B.C. Yang, Y.D. Hu, B.H. Wang, *Acta Chim. Sin.* 63 (12) (2005) 1127.

[137] V. Khomenko, E. Frackowiak, F. Beguin, *Electrochim. Acta* 50 (12) (2005) 2499.

[138] S. Talapatra, *Multifunctional Carbon Nanotubes-Introduction and Applications of Multifunctional Carbon Nanotubes*.

[139] R. Raccichini, A. Varzi, S. Passerini, B. Scrosati, *Nature Materials.* 14 (2015) 271.

[139] Y.Z. Chang, G.Y. Han, J.P. Yuan, D.Y. Fu, F.F. Liu, S.D. Li, *J. Power. Sour.* 238 (2013) 492.

[140] P. Chen, J.J. Yang, S.S. Li, Z. Wang, T.Y. Xiao, Y.H. Qian, *Nano. Energy*. 2 (2013) 249.

[141] Z. Li, J. Wang, S. Liu, X. Liu, S.Yang, J. Power. Sour. 196 (2011) 8160.

[142] Z. Zhang, F. Xiao, Y. Guo, S. Wang, Y. Liu, *ACS Appl. Mater. Interfaces*. 5 (2013) 2227.

[143] Y. Xu, X. Huang, Z. Lin, X. Zhong, Y. Huang, X. Duan, *Nano. Res*. 6 (2012) 65.

[144] X. Dong, Y. Cao, J. Wang, L. Wang, W. Huang, *RSC Adv*. 2 (2012) 4364.

[145] X. Dong, X. Wang, J. Wang, H. Song, X. Li, L.Wang, *Carbon*. 50 (2012) 4865.

[146] J. Yan, T. Wei, B. Shao, F. Ma, Z. Fan, M. Zhang, *Carbon*. 48 (2010) 1731.

[147] S. Ye, J. Feng, P. Wu, *ACS Appl. Mater. Inter.* 5 (2013) 7122.

[148] Y. Wang, S. Gai, N. Niu, F. He, P.Yang, *J. Mater. Chem*. A 1 (2013) 9083.

[149] Z.S. Wu, Y. Sun, Y.Z. Tan, S. Yang, X. Feng, K. Mullen, *J. Am. Chem. Soc*. 134 (2012) 19532.

[150] W. Wang, S. Guo, M. Penchev, I. Ruiz, K.N. Bozhilov, D. Yan, *Nanoscale*. 5 (2013) 6291.

[151] V. Sridhar, H.J. Kim, J.H. Jung, C. Lee, S. Park, I.K. Oh, *ACS Nano*. 6 (2012) 10562.

[152] A. Bello, K. Makgopa, M. Fabiane, A.D. Dodoo, K.I. Ozoemena, N. Manyala, *J. Mater. Sci.* 48 (2013) 6707.

[153] A. Bello, O.O. Fashedemi, M. Fabiane, J.N. Lekitima, K.I. Ozoemena, N. Manyala, *Electrochim. Acta*. 114 (2013) 48.

[154] W. Yang, Z. Gao, J. Wang, J. Ma, M. Zhang, L. Liu, *ACS Appl. Mater. Inter*. 5 (2013) 5443.

[155] G. Yu, L. Hu, M. Vosgueritchian, H. Wang, X. Xie, J.R. McDonough, *Nano. Lett*. 11 (2011) 2905.

[156] Y. Zhu, S. Murali, M.D. Stoller, K.J. Ganesh, W. Cai, P.J. Ferreira, *Science* 332 (2011) 1537.

[157] Z. Li, J. Wang, Z. Wang, H. Ran, Y. Li, X. Han, *New. J. Chem*. 36 (2012) 1490.

[158] L. Wang, D. Wang, J. Zhu, X. Liang, *Ionics* 19 (2012) 215.

[159] H.F. Huang, L.Q. Xu, Y.M. Tang, S.L. Tang, Y.W. Du, *Nanoscale*. 6 (2014) 2426.

[160] Y.M. He, W.J. Chen, X.D. Li, Z.X. Zhang, J.C. Fu, C.H. Zhao, *ACS Nano*. 7 (2013) 174.

[161] T. Zhai, F. Wang, M. Yu, S. Xie, C. Liang, C. Li, *Nanoscale*. 5 (2013) 6790.

[162] Y.J. Lee, H.W. Park, G.P. Kim, J. Yi, I.K. Song, *Curr. Appl. Phys*. 13 (2013) 945.

[163] L. Zhang, F. Zhang, X. Yang, G. Long, Y. Wu, T. Zhang, *Sci. Rep*. 3 (2013) 1408.

[164] H. Zhou, W. Yao, G. Li, J. Wang, Y. Lu, *Carbon*. 59 (2013) 495.

[165] W. Ouyang, J. Sun, J. Memon, C. Wang, J. Geng, Y. Huang, *Carbon*. 62 (2013) 501.

[166] Y. Zhao, J. Liu, Y. Hu, H. Cheng, C. Hu, C. Jiang, *Adv. Mater*. 25 (2013) 591.

[167] C. Zhao, X. Wang, S. Wang, Y. Wang, Y. Zhao, W. Zheng, *Int. J. Hydrogen. Energy*. 37 (2012) 11846.

[168] X. Dong, J. Wang, J. Wang, X. Li, L. Wang, *Mater. Chem. Phys*. 134 (2012) 576.

[169] Z. Tai, X. Yan, Q.Xue, *J. Electrochem. Soc*. A 159 (2012) 1702.

[170] K. Gao, Z. Shao, J. Li, X.Wang, X. Peng, W. Wang, *J. Mater. Chem.* A1 (2013) 63.

[171] Y. Han, M. Shen, Y. Wu, J. Zhu, B. Ding, H. Tong, *Synth. Met*. 172 (2013) 21.

[172] L. Li, J. Qiu, S. Wang, *Electrochim. Acta*. 99 (2013) 278.

[173] T.Y. Kim, G. Jung, S.Yoo, K. Suh, R. Ruoff, *ACS Nano*. 7 (2013) 6899.

[174] C. Huang, C. Li, G. Shi, *Energy. Environ. Sci*. 5 (2012) 8848

[175] Y. Zhu, L. Li, C. Zhang, G. Casillas, Z. Sun, Z. Yan, *Nat. Commun.* 3 (2012) 1225.

[176] H.L.Wang, Chris M. B. Holt, Z. Li, X.H. Tan, B.S.Amirkhiz, Z.W. Xu, B.C. Olsen, T. Stephenson, D. Mitlin, *Nano. Research*. 5 (2012) 605.

[177] K. Zhang, B.T. Ang, L.L. Zhang, X. S. Zhao and J.S. Wu, *J. Mater. Chem*. 2011, 21, 2663-2670

[178] J.C. Yoon, J.S. Lee, S.I. Kim, K.H. Kim, J. H. Jang, *Sci.Rep*. 3 (2013) 1788.